

N76-19181

9. THE PERFORMANCE OF COMPONENTS IN THE  
SKYLAB REFRIGERATION SYSTEM

By Charles E. Daniher, Jr.

Mc Donnell Douglas Astronautics Company

SUMMARY

The on-orbit performance of the Skylab Refrigeration System components is presented. Flight anomalies are analyzed and performance of the newly developed components is described.

Nine months of orbit data proved the practicality of the leak-free coolant system design. Flight-proven application of a thermal capacitor and development test results of the first all-mechanical, low-temperature mixing valve represent a significant advance in single-phase, low-temperature coolant loop design. System flight data suggest that additional instrumentation and fluid filters could have prevented system orbit performance anomalies.

INTRODUCTION

The Skylab Orbital Workshop (OWS) Module contained a refrigeration system (RS) that was designed to maintain  $0.248\text{m}^3$  (8.75 ft<sup>3</sup>) of frozen food at a temperature of  $250\text{ K} \pm 5.5\text{ K}$  ( $-10^\circ\text{F} \pm 10^\circ\text{F}$ ), freeze and maintain daily urine specimens (122 ml/crewman) at  $254\text{ K}$  ( $-2.5^\circ\text{F}$ ), chill daily micturition (4 liters/crewman) to less than  $288.2\text{ K}$  ( $59^\circ\text{F}$ ), and chil. water, medical supplies, and biological specimens to  $277\text{ K} \pm 3.3\text{ K}$  ( $39 \pm 6^\circ\text{F}$ ). Temperature control was initiated 40 days before the launch of Skylab 1 (April 17, 1974) and was maintained until the end of the last mission 307 days later (February 8, 1974).

The spatial location of RS equipment is shown in figure 1. A food freezer-chiller, located in the wardroom, and a water chiller, located in the wardroom table, are shown. The Bioanalysis Lab contained the urine freezer and chiller. The forward area (second floor) contained the food storage freezer, the RS pumps, and electronic control modules. The RS radiator and an insulated thermal control assembly that housed the thermal capacitors, flow control valves, and ground cooling heat exchangers were located on the aft end of the OWS.

The RS fluid schematic is shown in figure 2. Heat-transport and temperature control were accomplished by controlling the flow of a single-phase liquid coolant (Coolanol 15) through freezers and chillers. The heat picked up by the flowing coolant was either rejected (1) to the space environment through the zinc-oxide coated  $7.8\text{m}^2$  (84 ft<sup>2</sup>) radiator, (2) to the ground cooling heat exchanger during ground operation, or (3) to the thermal capacitor

0  
C  
e

during periods when the radiator or ground cooling heat exchangers were not operating (during launch and transient thermal orbit operation). Dual redundant coolant loops were employed to preclude a single system coolant leak that would result in the loss of RS cooling capability (reference 1).

Extensive knowledge and experience was obtained during the design of this low-temperature 244 K (-20°F), single-phase, liquid-coolant refrigeration system. The purpose of this paper is to present the design failures, successes, and recommendations resulting from flight experience, with the hope that future designs will not follow paths leading to failure but rather follow the paths to success. This paper is limited to the following four design areas:

1. Design of leak-free coolant systems.
2. Design of thermal capacitors and their usage in thermal feedback control systems.
3. Design of a thermostatically actuated, mechanical flow-control valve for low-temperature mixing.
4. Flight anomalies of flow and pressure control components and possible remedies.

## DESIGN OF LEAK-FREE COOLANT SYSTEMS

No detectable leakage of coolant, from either the primary or backup OWS RS cooling loops, showed in 307 days of ground and flight data (reference 1). In contrast, a similar redundant system on the Skylab leaked coolant from both loops and had to be refilled in flight. Neither the cause nor visible evidence of leaked coolant was found; however, the leaks were attributed to mechanical connections. The RS leak data show that it is possible to design a leak-free system. The suggestion is made that this leak-free performance resulted from the use of high quality fluid fittings and the application of stringent test criteria.

### Design Philosophy and Hardware

The following discussion outlines the philosophy and hardware used in the RS design.

1. Minimize all mechanically separable connectors by brazing system coolant connections.
2. Where separable connections are required, use high-quality MC (Marshall Center) specifications for tube fittings, flares, O-rings, and K-seals.

3. Leak test braze fittings to  $1 \times 10^{-6}$  sccs He at 930.69 kPa (135 psig) and leak test mechanically separable connectors to  $1 \times 10^{-5}$  sccs as determined by mass spectrometer quantitative analysis.
4. Retorque B-nut connectors after pressure cycling to minimize the possibility of torque relaxation.

A typical braze union is shown in figure 3. The union was made of 340L CRES cond A. The braze material was 82-percent gold and 18-percent nickel and was held in the braze union bulb until melted out. A prime consideration was the effect of the melting temperature on components as a result of the required fitting brazing temperature of 1,311 K (1,900°F) for 35 sec. Testing revealed that the MC266J fluorosilicone rubber seal reached 394.3 K (250°F) during the braze operation; the seal can maintain its effectiveness to 505.4 K (450°F).

Mechanically separable connections to off-the-shelf hardware and to removeable equipment were made using either the braze adapter shown in figure 3, which was sealed with a fluorosilicone packing or a teflon-coated metal-K seal, or an MC flare tube connector shown in figure 4.

Leak testing of each coolant loop was accomplished using 930.69 kPa (135 psig) helium to a level of  $10^{-5}$  sccs per joint. Care was taken to ensure that joints leak-checked with gas were dry and free of capillary liquid which could block potential leak paths. The system was also leak-checked by a pressure decay test with a decay of -0.124 kPa/hr (0.5 in H<sub>2</sub>O/hr) allowable, using 930.69 kPa (135 psig) helium.

The RS contained a total of 413 joints of which 253 were braze fittings, 112 were O-rings or K-seals and 48 were MC flare fittings.

#### Leak Prediction

##### Symbols

- P = pressure
- V<sub>G</sub> = maximum gas volume when accumulators are empty
- K<sub>B</sub> = effective metal bellows spring rate
- X<sub>0</sub> = bellows preload
- A<sub>B</sub> = effective bellows piston area
- M<sub>G</sub> = mass of accumulator gas charge
- R<sub>G</sub> = gas constant
- T<sub>G</sub> = absolute gas temperature
- V<sub>A</sub> = volume of coolant in accumulator

$V_S$  = volume of coolant in one system loop with accumulator empty

$M_L$  = mass of liquid coolant loaded into system

$\bar{T}_L$  = average coolant temperature

$\rho_L$  = density of liquid coolant

$C_i$  = mass weighting constants

$\epsilon$  = pressure error

Subscript

L = liquid coolant

G = accumulator gas

B = metal bellows

S = per coolant loop

The prediction of flight coolant leakage was a mission data requirement. It is a paradox that leak-tight systems may not allow for the prediction of an unacceptable leak rate because of low gains on the measured parameters necessary to predict leakage.

$$\left( \text{i. e., low } \frac{\partial P_L}{\partial V_A} \text{ or low } \frac{\partial V_A}{\partial T_L} \right)$$

For example, the random error on the RS pressure measurements were such that 66 days were required to determine if a temperature-corrected pressure was actually a leak.

The off-the-shelf coolant accumulators did not incorporate a direct reading volume indicator. Thus, the volume of coolant had to be indirectly determined from the pressure on the coolant and the temperature of the accumulator gas. Pressure was maintained on the liquid coolant by a spring-loaded metal bellows and a non-condensing R-22 gas (figure 5).

The leak calculation procedure was to determine what the pressure on the coolant should be. This calculated pressure was then compared with the actual flight pressure and a pressure error number generated:

$$P_{\text{FLIGHT}} - P_C = \epsilon \quad (1)$$

The pressure on the coolant is described by

$$P_C = \underbrace{K_S X_o}_{\text{metal bellows preload}} + \underbrace{\frac{K_S V_A}{A_p^2}}_{\text{pressure due to bellows compression}} + \underbrace{\frac{M_G R_G T_G}{V_G - V_A}}_{\text{pressure due to accumulator gas}} \quad (2)$$

All leak detection schemes must assess the average coolant temperature to determine the volume of the coolant in the system and hence the amount of coolant that should be in the accumulator. The average coolant temperature is found from:

$$\bar{T}_L = \sum_{i=1}^n C_i T_i \quad (3)$$

$C_i$ 's are mass-weighting constants. The RS coolant volume was divided into 16 isothermal nodes represented by combinations of flight temperature transducers (figure 5).

The volume of coolant in the accumulator was found from:

$$V_a = \frac{M_L}{\rho(\bar{T}_L)} - V_S \quad (4)$$

The leak calculation procedure is as follows:

1. Determine the average coolant temperature from equation (3).
2. Calculate the volume that should be in the accumulator from equation (4).
3. Calculate the coolant pressure using equation (2).
4. Calculate the pressure error using equation (1).

The mission leak-prediction results are shown in figure 6, with pressure error plotted against the day of the year (DOY).

Data evaluations were started on DOY 134 (May 14, 1973). The average value of the pressure error ( $\mu$ ) of 20.5 kPa (2.967 psig) was a systematic error that was probably due to variations in metal bellows spring constants  $K_S$ , the magnitude of the gas charge  $M_G$ , and uncertainty in coolant fill mass  $M_L$ .

The lower bound of measurement tolerance was established by adding the pressure transducer least bit error 2.14 kPa (0.31 psig) to the transducer

0  
C  
E

repeatability 2.07 kPa (0.3 psig). The allowable system leakage 197 cm<sup>3</sup>/year (12 in.<sup>3</sup>/year) was equivalent to a pressure decay of 0.0517 kPa/day (0.0075 psig/day). Figure 6 shows that no coolant leakage was detectable.

As a result of the difficulty in measuring system leakage, it is recommended that future systems either incorporate a high-gain accumulator (large  $\partial P/\partial VA$ ) or incorporate volume-indicating instrumentation and provide sufficient temperature instrumentation to determine the average liquid temperature. Depending upon margins, the evaluation of possible leaks could be substantially reduced from the 66-day Skylab RS limit.

## DESIGN AND USAGE OF THERMAL CAPACITORS

The RS used a phase-changing heat sink (thermal capacitor) as a heat storage device. Heat was transported to and from the liquid coolant that flowed through it at a constant rate of 56.7 kg/hr (125 lb/hr).

The phase-change material (PCM) was Undecane (C<sub>11</sub> H<sub>24</sub>), a polymorphic odd-numbered paraffin with a liquid/solid fusion point at 247.60 K (-14°F) and a crystal structure change at 236.5 K (-34°F) (reference 2). At 247.60 K, the capacitor stored 36.68 cal/gr (56 Btu/lb); at 236.5 K it stored an additional 10.01 cal/gr (18 Btu/lb).

### Design of Capacitors

The thermal capacitor was fabricated in three identical segments and plumbed in series as shown in figure 2. The construction of each segment is shown in figure 7 and consisted of:

1. A plate fin coldplate which transported heat between the coolant and the coldplate surface.
2. A PCM chamber which contained and allowed for expansion and contraction of the PCM, and transferred heat between the coldplate and the PCM.
3. A PCM that changes phase at 247.6 K (-14°F).

The PCM chamber was a special hex cell or honeycomb design. The hex cells were 0.3175 cm (1/8 in) across the flats and 2.54 cm (1 in) tall with 0.015-cm- (0.006-in) thick aluminum foil walls (figure 7C). Small cell size was desired to increase the effective thermal conductance to the PCM. Each hex cell was filled 80 percent with PCM and 20-percent air for ullage, (figure 7B). The ends of the hex cells were bonded to aluminum sheets, one end to the coldplate surface and the other to a thin sheet of aluminum.

The design captured a discrete expansion (ullage) volume into each cell. This was required because the wax volume increased 8 percent when melted. The original design did not capture the ullage but simply allowed for a

20-percent expansion in a chamber with open cell tops. When this original unit was slightly tilted and melted, the wax chambers ruptured. In zero gravity this same effect would result due to the Marangoni effect which observes that liquid will tend to flow towards regions of high surface tension (low temperature) (reference 2).

#### Capacitor Use in Thermal Feedback Control System

The thermal capacitor (TC) provided a means to filter cyclic inlet temperatures from the space radiator of  $244.26 \text{ K} \pm 15 \text{ K}$  ( $-20 \pm 27^\circ\text{F}$ ) to a cyclic amplitude of  $242 \text{ K} \pm 4.4 \text{ K}$  ( $-24^\circ\text{F} \pm 8^\circ\text{F}$ ) at the outlet of the third segment (figure 8).

The capacitor also provided deadband for the feedback controller. A temperature sensor located on the coolant tube downstream of the first capacitor segment (figure 2) was used to control the radiator bypass valve and maintain the two downstream thermal capacitor segments in a frozen state.

When the TC control temperature sensor reached  $248.26 \text{ K}$  ( $-12.8^\circ\text{F}$ ), indicating that the first segment had melted, the coolant flow was diverted to the radiator and the capacitor refrozen. Cooling was terminated when this same TC sensor reached  $236.21 \text{ K}$  ( $-34.5^\circ\text{F}$ ) at which time coolant flow was bypassed around the radiator and the first segment would then begin to melt again. This deadband resulted in a 93-minute limit cycle. The system response, (figure 8), shows the coolant temperature out of the third TC segment was maintained at less than  $247.59 \text{ K}$  ( $-14^\circ\text{F}$ ), the PCM fusion point.

Designers of future systems should consider liquid-coupled thermal capacitors as flight qualified components. Their effective use can greatly reduce the required radiating area and make possible the design of low-temperature refrigeration systems. In addition, capacitors provide substantial temperature filtering; they also provide their own controller deadband. The large thermal expansion and low thermal conductivity PCM's require a design of small hexagonal cells  $0.32 \text{ cm}$  by  $2.54 \text{ cm}$  ( $1/8\text{-in}$  by  $1\text{-in}$ ) to increase the thermal conductance to the wax and with captured ullage to minimize the PCM expansion yield path to ullage.

#### LOW-TEMPERATURE FLOW CONTROL VALVE DEVELOPMENT

A thermostatically actuated flow control valve was developed to proportionally control flow through the radiator and thermal capacitor as shown in figure 9B. Proportional flow control was selected to meet an original requirement to limit frozen food temperature cycle amplitude. Flow and temperature instability showed up at the component test level; the proportional control valve was replaced with a binary flow control system and consequentially was not part of the RS. However, the oscillation (instability) problems were solved by degaining the valve area/stroke function at the hot port. Completion on this modification was too late to meet the Skylab launch schedule.

0  
C

Degaining increased the stroke required to close the hot port and resulted in an increase in the valve control temperature bandwidth from  $244.26 \pm 1.66$  K ( $-20 \pm 3^\circ\text{F}$ ) to  $247$  K  $\pm 3.3$  K ( $-15 \pm 6^\circ\text{F}$ ). Although this performance did not meet the tolerance limits originally specified, this is the first flight-type, thermally-actuated valve to be developed for this low-temperature operating band. The low temperature flow control valve is shown in figure 9A. The total dry weight was 2.19 kg (4.84 lb), the length 25.4 cm (10.0 in), and the diameter 4.8 cm (1.89 in). This design functioned as follows:

An actuation medium, consisting of silicone fluid (DC-200) doped with (20 percent by volume) copper flake to improve thermal conductivity, was contained within an internally and externally finned actuator housing. The actuation medium linearly expanded and contracted, on heating and cooling respectively, as a function of the valve coolant mix temperature. This medium volume change was amplified and converted to a linear stroke by moving a bellows-sealed piston. The piston was connected to a slotted sleeve that masked and controlled the hot and cold coolant fluid passage openings. The fully open hot to fully open cold piston travel was 0.0889 cm (0.035 in). This travel took place between a  $244.26$  K ( $-20^\circ\text{F}$ ) to  $247.59$  K ( $-14^\circ\text{F}$ ) change in the actuation medium temperature. Over-temperature protection was provided by a second over-travel piston sealed by an over-travel bellows. This piston moved off its mechanical stops after the slotted sleeve had moved to the far left limiting position. Over-temperature protection to  $322.03$  K ( $+120^\circ\text{F}$ ) was provided.

Early problems developed during valve testing. The actuation bellows squirmed, causing a shift in the temperature control band. The problem was solved by a hardware change using a close tolerance teflon guide cylinder for the bellows.

The valve also exhibited a temperature control instability with an amplitude of  $8.33$  K ( $15^\circ\text{F}$ ) and a period of 24 seconds. Instability was found to be a function of the radiator pressure drop and the difference in the hot and cold port temperatures. In the above case, instability occurred when the cold port temperature was  $210.9$  K ( $-80^\circ\text{F}$ ), the hot port was  $250.37$  K ( $-9^\circ\text{F}$ ), and the radiator pressure drop was  $275.76$  kPa (40 psid). This pressure drop had to be balanced by the hot-port, slotted-sleeve opening. The problem was the high area change to stroke gain at bypass port closure. The solution was to degain the bypass port by taking more valve stroke to change the port area from full open to full closed. The resulting performance is shown in figure 10 (reference 3). The condition being run was a simulated radiator temperature change at a high radiator pressure drop of  $344.7$  kPa (50 psid); minimum radiator temperature was  $210.9$  K ( $-80^\circ\text{F}$ ); and the bypass temperature was  $266.48$  K ( $+20^\circ\text{F}$ ). As a result of this valve development, the following design recommendations are made:

1. Define port "load lines" early (pressure drop versus flow characteristics). If the evolving design is in such an unpredictable state (final radiator size not known), then a valve installation as shown in figure 9C should be considered. The maximum pressure drop imbalance is controlled by the design of the regenerator heat exchanger only. This approach was used successfully for the chiller valve shown in figure 2. When selected, the regenerator heat

exchanger approach allows the flow control valve development to proceed independent of the final radiator design.

2. Component-level testing should realistically simulate the flight system characteristics and should include the following:

Test conditions, that force the valve to perform its control function at the end of its stroke (at port closure), should be selected for stability analysis. For example: the coldest bypass port temperature 249.82 K (-10°F), the coldest radiator port temperature 210.93 K (-80°F), and the highest radiator pressure drop 310.23 kPa (45 psid) all combine to force the valve to flow control on the bypass port.

Testing should also include conditions that simulate the inlet port temperature design limits; this may reveal a fluid mixing instability. For example: this valve was tested with a bypass port temperature of 266.48 K (+20°F) and a radiator port temperature of 205.37 K (-90°F).

Testing should include the simulation of expected inlet temperature and pressure ramps to determine valve mix temperature tracking limits.

Data required for valve math modeling are:

1. Actuator stroke versus temperature (note bellows actuators usually have a hysteresis which provides deadband).
2. Port orifice coefficients versus stroke.
3. Actuator thermal time constant and effective capacitance.

#### FLIGHT ANOMALIES OF FLIGHT FLOW AND PRESSURE CONTROL COMPONENTS

The RS binary radiator flow control system functioned normally as shown in figure 8 until anomalous performance was observed on DOY 173. The expected and actual flight performance of the thermal capacitor outlet temperature and the coolant system differential pressures are shown in figure 11.

#### Description of Anomaly

At approximately 17:02:03 GMT, the system differential pressure decreased 34.47 kPa (5 psid), at a time when a switch to radiator flow was expected, due to a 248.26 K (-12.8°F) thermal capacitor control sensor signal. The expected differential pressure was 392.96 kPa (57 psid) which indicated that warm fluid was being diverted through a viscous radiator. The low differential pressure of 220.6 kPa (32 psid) and thermal capacitor inlet

temperature of 255.37 K (0°F) suggested that total flow was not flowing through the radiator and that a split flow (radiator and/or bypass legs path A and B, figure 2) was occurring.

The complete melt of the thermal capacitor occurred approximately 2 hours after the anomaly and an automatic switch to the backup coolant loop, caused by a food temperature sensor exceeding 255.93 K (+1°F), resulted in even worse performance. Apparently the secondary loop was also bypassing coolant flow around the radiator.

The potential leak paths are shown in figure 2. A leak through path B is caused by coolant flow past the bypass port poppet of the radiator bypass valve (RBV). Subsequent investigation indicated that a 25 $\mu$  particle, if trapped in the poppet seat, could cause the observed leak. Path A is through the radiator relief valve which could have lodged open due to contamination. Continuous cycling of the RBV by ground controllers may have been the cause for performance improvement since the RS primary loop returned to an acceptable split-flow performance mode (approximately 50 hours after the anomaly) and continued to function until the end of the last mission (February 8, 1974). The binary flow control system was disabled and the RBV left in the radiator flow position at that time.

#### Probable Causes and Recommendations

This anomalous performance might be prevented in future designs if the following two recommendations are implemented.

The first recommendation is to provide for particle filtering upstream of all valves that are contamination sensitive, and especially if they are located downstream of brazed heat exchangers. The brazed plate fin regenerator heat exchanger shown in figure 2 was a likely candidate for particle generation. This was assumed since vibrations and zero gravity could coincide to loosen and allow braze particles to enter the coolant flow stream. Better cleaning practices may reduce the number of particles generated but the judgement is that brazed heat exchangers will always be a potential source of particles large enough to cause a valve malfunction of the type observed.

The second recommendation is to provide a simple flow-sensitive reed switch to be located at points A and B (figure 2) and set to indicate flows above the allowable leakage values (in this case flows  $\geq 0.91$  Ks/Hr ( $\geq 2$  lb/hr). This would allow for the positive ground checkout of the full radiator flow function. In retrospect, ground checkout procedures and existing instrumentation did not allow for the accurate determination of the full radiator flow condition when the RBV was commanded to the radiator flow position. Accurate assessment of the full bypass position was accomplished by noting the thermal capacitor inlet temperature when the ground cooling heat exchanger was operating. A partial flow of 259.26 K (+7°F) coolant to the radiator would have resulted in (1) condensation on the radiator surface and (2) a thermal capacitor inlet temperature higher than the coolant temperature out of the ground-cooling heat exchanger. The assessment of

the full radiator flow could not be determined in the same manner. Rather, it was determined by changes in system differential pressure between radiator and bypass RBV positions.

#### CONCLUDING REMARKS

Designers of future coolant systems should carefully evaluate cleaned heat exchangers as potential contamination sources and provide for coolant particle filtration. In addition, allowance should be made in the system for the incorporation of instrumentation, such as the flow-actuated reed switches, to verify required full and no-flow conditions.

#### REFERENCES

1. Skylab Final Technical Report. McDonnell Douglas Report MDC-G5170, May 1974.
2. Phase Change Materials Handbook. Interim Development Test Report, Nasa Report CR-61363, September 1971.
3. Radiator Control Valve. AiResearch Manufacturing Co., Report 72-8475, August 9, 1972.

#### ACKNOWLEDGMENT

The work discussed in this paper was sponsored by NASA Marshall Space Flight Center and Johnson Space Center under Contract NAS9-6555.

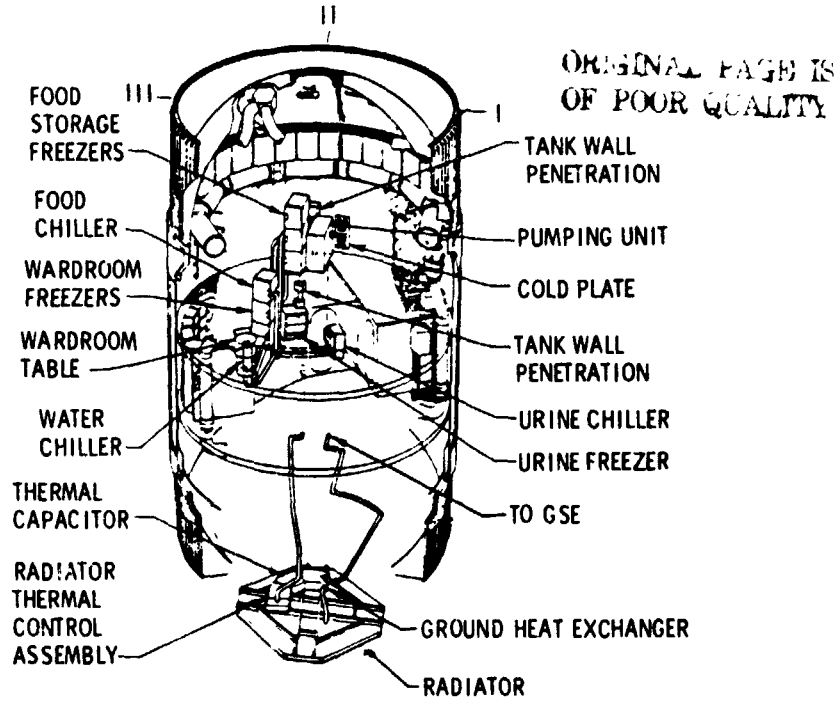


Figure 1. Skylab Orbital Workshop Refrigeration System

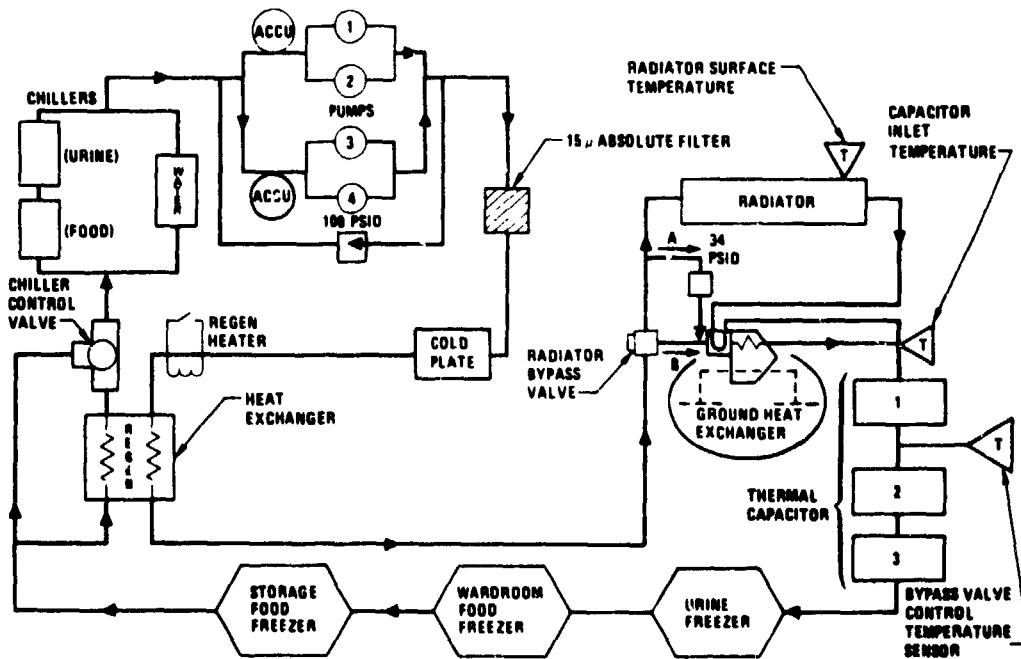


Figure 2. Refrigeration System Fluid Schematic

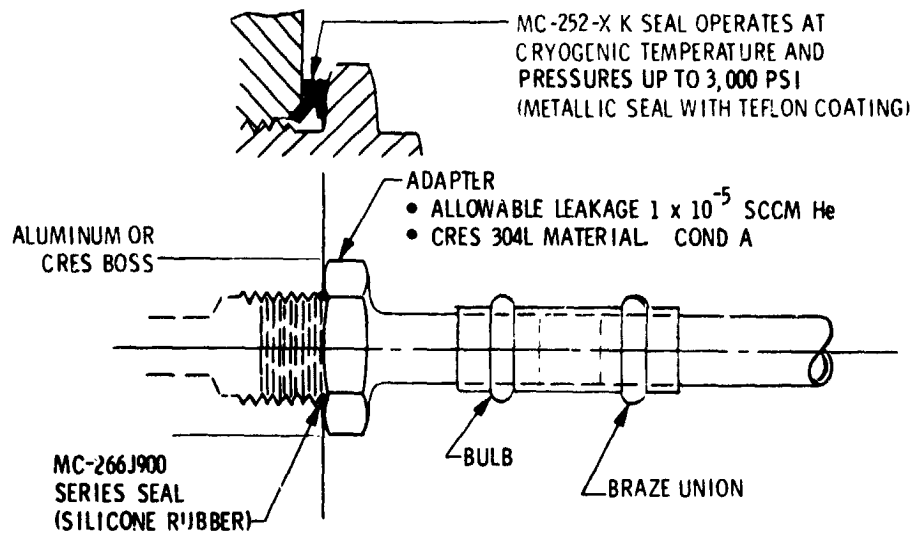


Figure 3. Refrigeration System Component-to-Boss Fluid Connection

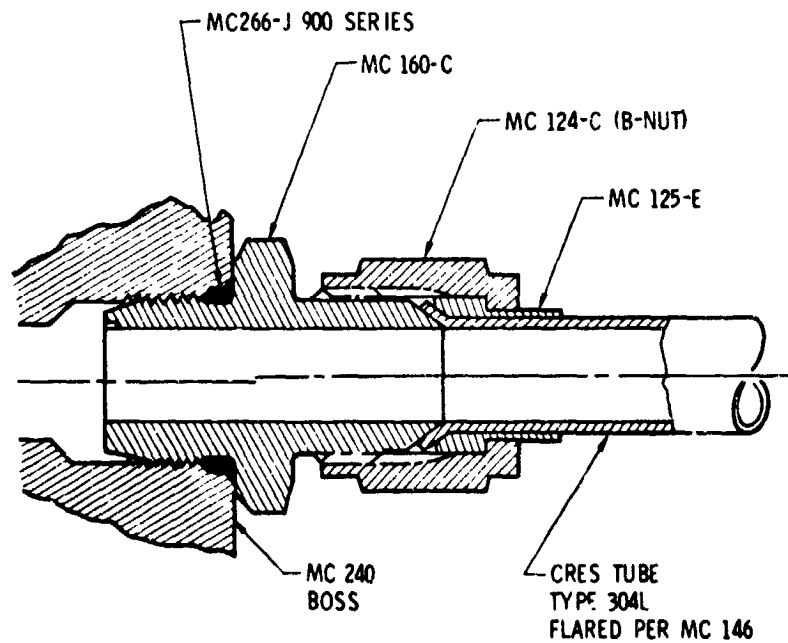


Figure 4. Refrigeration System Flare Tube Connector (MC)

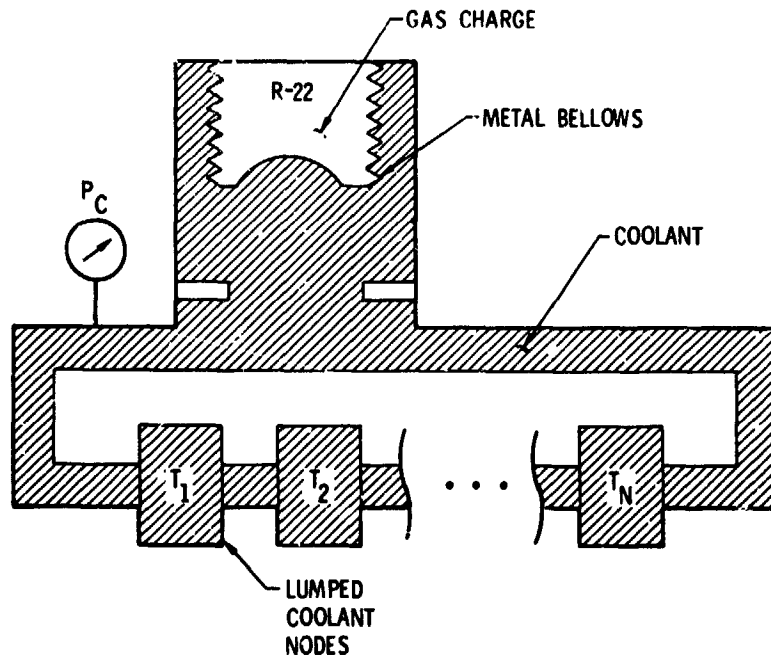


Figure 5. Refrigeration System Symbolic Coolant Loop

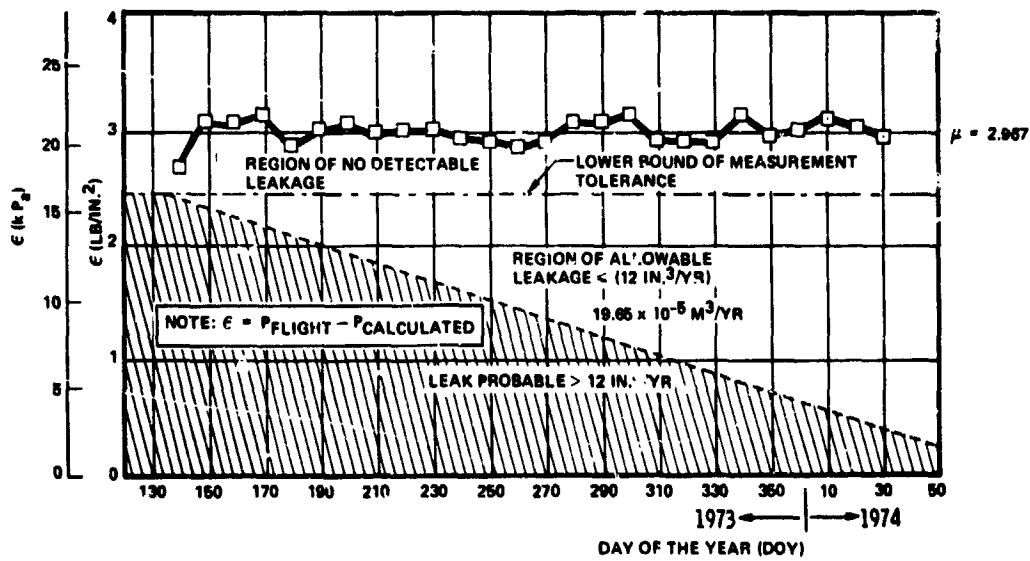


Figure 6. Refrigeration System Primary Loop Leakage 10-Day Averages

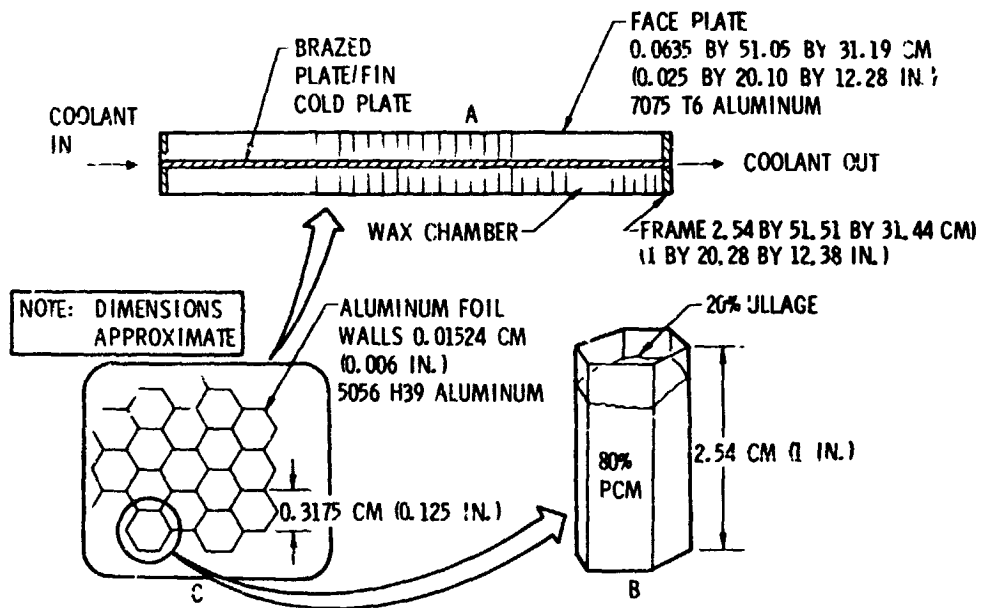


Figure 7. Refrigeration System Thermal Capacitor Segment

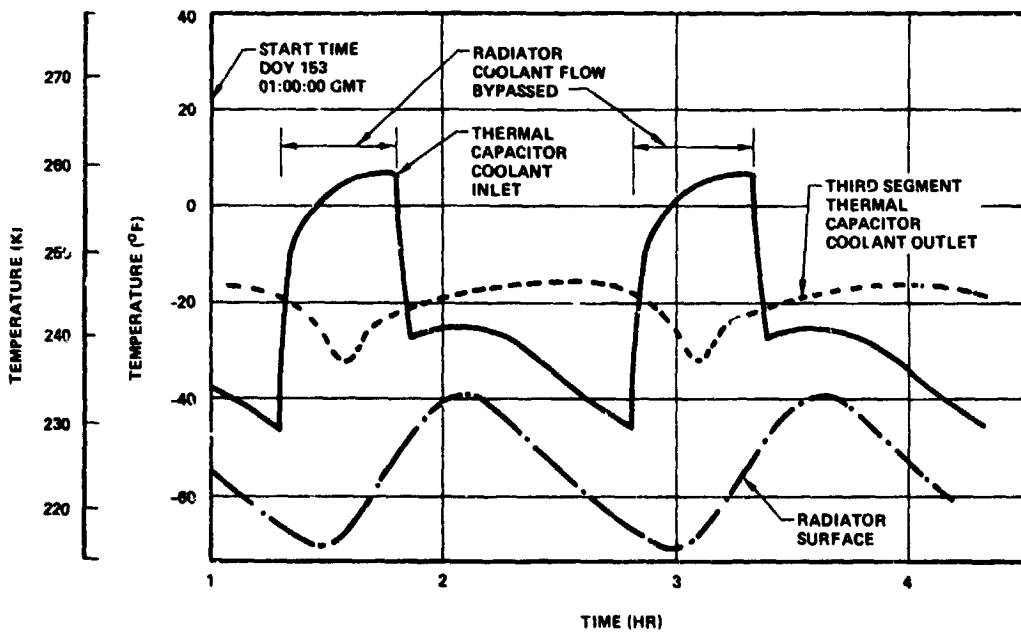


Figure 8. Refrigeration System Thermal Capacitor Performance Temperatures

ORIGINAL PAGE IS  
OF POOR QUALITY

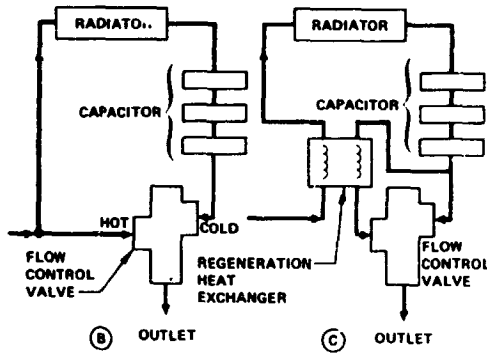
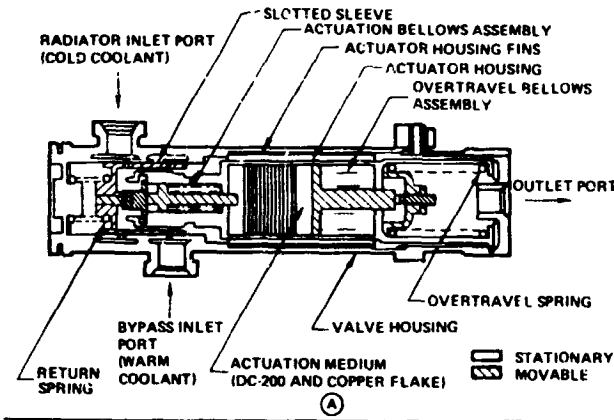


Figure 9. Low-Temperature Flow Control Valve

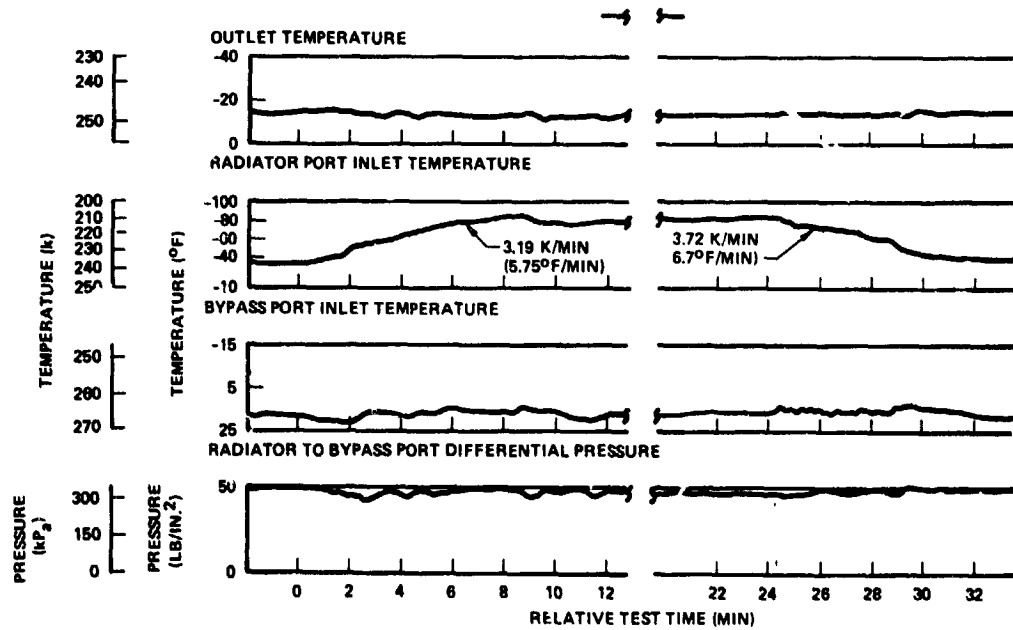


Figure 10. Radiator Control Valve Performance Maximum Hot Port Differential Pressure

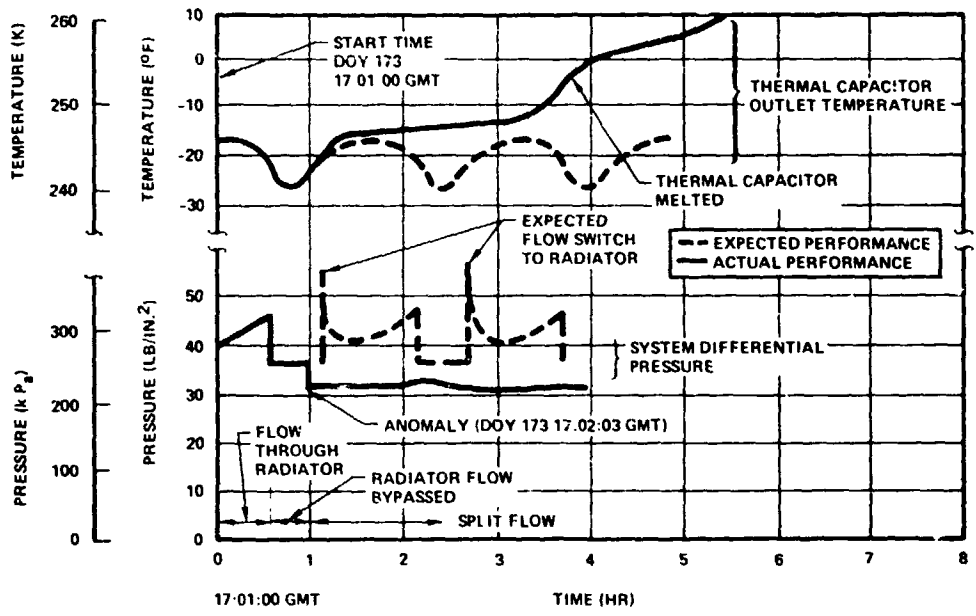


Figure 11. Refrigeration System Performance Anomaly

ORIGINAL PAGE IS  
OF POOR QUALITY